JOURNAL OF CATALYSIS 54, 129–142 (1978)

Surface Area Stabilization of Ir/Al_2O_3 Catalysts by CaO, SrO, and BaO Under Oxygen Atmospheres: Implications on the Mechanism of Catalyst Sintering and Redispersion

G. B. McVicker, R. L. Garten, and R. T. K. Baker

Exxon Research and Engineering Company, Corporate Research Laboratories, P.O. Box 45, Linden, New Jersey 07036

Received January 12, 1978; revised April 3, 1978

An approach for preventing sintering and maintaining high metal dispersions of Ir/Al_2O_3 catalysts in the presence of oxygen at elevated temperatures has been developed. Well-dispersed Ir/Al_2O_3 catalysts were readily sintered under oxygen at temperatures above 450°C. If, however, Ba, Ca, or Sr oxides were impregnated onto the Al_2O_3 support along with the Ir, then complete inhibition of sintering was observed up to 650°C. This effect only occurred when the concentration of Ba, Ca, or Sr oxides was in excess of the concentration of acid sites on the Al_2O_3 support. Studies of presintered Ir/Al_2O_3 catalysts to which BaO was subsequently added demonstrated that Ir could be redispersed by treating the system with oxygen at 600°C. The oxidative stabilization and redispersion of Ir/Al_2O_3 catalysts are consistent with the capture of mobile, molecular, iridium oxide species by well-dispersed Group IIA-oxide sites. The trapping mechanism is assumed to proceed via the formation of stable, immobile surface iridates.

INTRODUCTION

Supported noble metal catalysts are used in a wide variety of industrially important hydrocarbon conversion reactions (*1*). Such catalysts consist in general of small metal crystallites dispersed over and within the pore structure of high surface area metal oxide supports (*2*). In the absence of specific poisons such as sulfur, arsenic, and heavy metals, hydrocarbon conversion catalysts deactivate with time as a result of coke deposition. Catalyst regeneration is achieved by combusting the coke deposit in an oxygen-containing atmosphere at temperatures near 500°C. The combustion process, however, causes an increase in the average metal crystallite size (*3*). The resulting loss in metal surface area generally leads to decreases in catalytic activity and in some instances to changes in product selectivity patterns (*4–5*).

The mechanism by which supported metal crystallites sinter is currently generating considerable interest (*6–10*). Two models have recently appeared in the literature which account, with differing degrees of success, for the sintering behavior of supported metal catalysts. One model, proposed by Ruckenstein and Pulvermacher, envisages sintering by crystallite migration followed by collision and fusion into larger crystallites (*11*). Wynblatt and Gjostein have strongly suggested that crystallite migration is energetically restricted to metal crystallites smaller than 50 Å in diameter (*12*). During the initial stages of sintering of well-dispersed metal catalysts crystallite migration may occur,

0021-9517/78/0542-0129$02.00/0

but the process is disfavored after extensive sintering where larger crystallites are present. Under certain reaction conditions sintered Pt catalysts have been observed to redisperse (*13*). In the absence of a crystallite fragmentation process, redispersion via crystallite migration cannot be readily rationalized. The second model, commonly referred to as the atomic or molecular migration model, has been developed by Flynn and Wanke as an extension of classical Ostwald ripening mechanisms (*14*). They propose that sintering occurs by the surface transport of dissociated atomic or molecular species which ultimately collide with and are captured by a second larger stationary metal crystallite. The overall process results in the growth of larger crystallites at the expense of smaller crystallites. Such behavior is predicted by the Kelvin equation, which suggests that the rate of loss of atoms is lower than the rate of capture for large crystallites, whereas for small crystallites the rate of loss is higher than the rate of capture (*15*). The driving force for molecular transport is the minimization of surface free energy. The atomic migration model can account for the buildup in concentration of small transporting particles on the support surface. In the case where the rate of generation of molecular species is higher than their rate of capture a net redispersion is possible. Sintering by either an atomic or crystallite migration mechanism will be highly temperature dependent; the former process, however, would certainly be more strongly influenced by the sintering atmosphere and support interactions (*16–18*).

We suggest that under oxygen atmospheres sintering by either crystallite or atomic particle migration may be suppressed or eliminated if a chemical trap is present on the support surface. This proposal is illustrated in Fig. 1. In the absence of crystallite fracturing no net redispersion would be predicted by the capture of migrating crystallites. In the case of an atomic or molecular migration a chemical trap could lead to redispersion. The use of chemical trapping agents may then provide a means of differentiating between the contrasting sintering models.

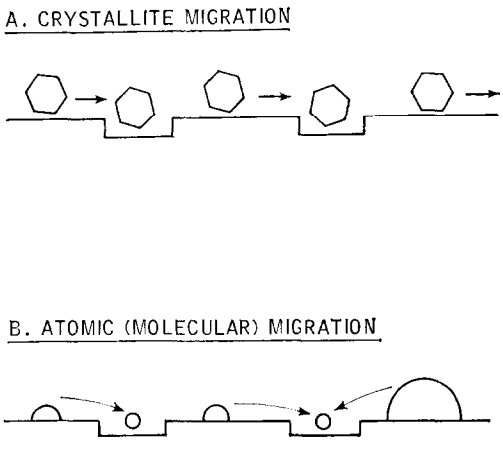

FIG. 1. Schematic representation of the effect of a chemical trap on the two proposed mechanisms of particle sintering. (A) Redispersion not predicted by crystallite migration model. (B) Redispersion possible by atomic migration model.

For our studies we have elected to investigate the sintering behavior of Ir/Al_2O_3 catalysts under oxygen atmospheres. Iridium catalysts were chosen since preliminary studies showed Ir to sinter at much lower temperatures than required for Pt/Al_2O_3 catalysts. The lower sintering temperatures required for Ir eliminate potential ambiguities brought about by structural transformations of the Al_2O_3 support (*19*).

Iridium in the presence of oxygen is known to form thermally stable iridates ($MIrO_3$) with the oxides of Ca, Sr, and Ba (*20, 21*). Magnesium, because of its smaller ionic radius, does not form a stable iridate (*22*). TGA measurements have shown that Ca, Sr, and Ba iridates are reduced under hydrogen within the temperature range of 350 to 450°C (*23*). The reduction products are Ir metal and the corresponding Group IIA-oxide. The ready formation of stable Group IIA iridates under oxygen and their ease of reduction suggest the usage of

Group IIA-oxides as chemical trapping agents for Ir/Al_2O_3 catalysts.

In this paper experimental measurements of the oxidative growth and redispersion of Ir supported on Al_2O_3 and Group IIA-oxide doped Al_2O_3 carriers are presented and discussed. Sintering and redispersion rates were determined by a combination of X-ray diffraction, chemisorption, transmission electron microscopy (TEM), and controlled atmosphere electron microscopy (CAEM) measurements on both conventional and model supported Ir catalysts. These studies have shown CaO, SrO, and BaO doped Al_2O_3 supports completely inhibit the oxidative sintering of Ir at temperatures up to 650°C. Presintered Ir/Al_2O_3 catalysts to which was added a BaO surface phase were observed to redisperse under oxygen when heated to 600°C. Both the oxidative sintering suppression and oxidative redispersion of Ir are consistent with the capture of a mobile, molecular, iridium oxide species by a Group IIA-oxide chemical trap. The trapping mechanism is assumed to proceed via the formation of a stable surface Group IIA-metal iridate.

EXPERIMENTAL METHODS

Materials

Al_2O_3 and group IIA-oxide doped Al_2O_3 supports. η-Al_2O_3 was prepared by calcining β-alumina trihydrate in air for 16 hr at 600°C. Group IIA-oxide doped Al_2O_3 supports were prepared by incipient wetness impregnation of η-Al_2O_3 with Group IIA-metal nitrate salts (in the case of Ba the more soluble nitrite salt was employed). The impregnates were dried for 16 hr at 120°C and then calcined in dry air for 16 hr at 600°C to ensure complete decomposition of the nitrate (nitrite) salts.

Supported metal catalysts. Platinum and iridium catalysts were prepared by incipient wetness impregnation of η-Al_2O_3 and Group IIA-oxide doped η-Al_2O_3 supports with analyzed aqueous solutions of chloroplatinic and chloroiridic acids (0.1 g of metal/ml). The impregnates were dried in dry air for 16 hr at 120°C and then mildly calcined in dry air at 270°C for an additional 4.0 hr. Metal analyses were found in all cases to be in excellent agreement with the nominal values (*24*).

Model supported metal catalysts. Model supported catalysts employed in TEM and CAEM studies were prepared as follows: High-purity aluminum foil was thoroughly cleaned and then anodized in an electrolyte containing sodium hydrogen phosphate, sulfuric acid, and water, so that a thin film of oxide was built up on the metal surface. The conditions required to obtain a good quality γ-Al_2O_3 film, approximately 500 Å in thickness, were extremely critical, the best results being obtained at 30 V for 7 sec. The oxide film was subsequently released from the unconverted metal by dissolving the latter in 50% HCl. This step was repeated several times with fresh acid to ensure that all traces of free metal were removed. The films were finally washed in deionized water. Iridium and barium were introduced onto the γ-Al_2O_3 films as atomized sprays of 0.1% aqueous solutions of chloroiridic acid and barium nitrite.

Equipment and Procedures

Sintering treatments. Oxidative calcinations of conventional as well as model catalysts under 1 atm total pressure were carried out by one of the following procedures: (i) calcining under dry air in a muffle furnace, (ii) calcining under dry air or 20% O_2/He flowing at 500 cc/min in a tube furnace, or (iii) calcining under dry air (200–500 cc/min) in a gas adsorption cell. Catalysts were generally prereduced at the calcination temperature.

Chemisorption measurements. Hydrogen and carbon monoxide chemisorption studies were performed with a conventional glass vacuum system. The system incorporated

an 80-liter/min oil diffusion pump backed by a mechanical pump with liquid nitrogen traps on the inlet and outlet of the diffusion pump. Ultimate dynamic vacuums of about 10^{-7} Torr were obtainable. Pressure measurements during chemisorption studies were made with a Texas Instruments Precision Pressure gauge. Samples of 1 to 4 g, sieved to 20- to 40-mesh size, were placed into flow-through cells made of Vycor. Samples were reduced at 500°C under hydrogen (500 cc/min) *in situ* for 1 hr. The reduced samples were cooled to 450°C under hydrogen and evacuated at this temperature for 0.5 hr. The sample was then cooled under dynamic vacuum to room temperature. Longer reduction and evacuation times did not affect the chemisorption results.

Hydrogen and carbon monoxide uptakes were determined at 25 ± 2°C on the reduced and evacuated samples. Typically, 30 to 60 min was allowed for each uptake point. The H/M ratios were calculated by assuming that H_2 uptakes at zero pressure of H_2 corresponded to saturation coverage of the metal. These uptakes were determined by extrapolation of the high-pressure linear portion of the isotherm, as described by Benson and Boudart (*25*) and Wilson and Hall (*26*). The CO/M ratios were calculated by determining the CO uptakes on the reduced and evacuated samples and assuming that this represented the sum of CO weakly bound to the support and strongly bound to the metal. The sample was then evacuated for 10 min at room temperature, and a second CO isotherm was measured. Since the second isotherm measures only the CO weakly adsorbed on the support, subtraction of the two isotherms gives the amount of strongly bound CO which is associated with the metal. In accordance with previous studies (*27*), the amount of strongly bound CO at 100 Torr pressure was chosen as saturation coverage of the metal.

BET surface area measurements were determined with argon at liquid nitrogen temperature. A value of 14.6 Å^2 was assumed for the area of an argon atom and a value of 210 Torr was used for P_0.

Hydrogen of 99.95% purity was passed through a Deoxo unit (Engelhard Industries, Inc.), a 5 A molecular sieve drying trap, an Oxy-trap (Alltech Associates, Arlington Heights, Illinois) to remove last traces of oxygen, and finally through a liquid nitrogen trap before being admitted to the catalyst for reductions or chemisorption measurements. Carbon monoxide of 99.99% purity was passed through a dry ice–isopropanol trap before exposure to the sample. Argon of 99.9995% purity was used as received.

X-Ray diffraction measurements. A Philips Electronics X-ray diffractometer (XRG-3000) with nickel-filtered Cu–Kα radiation was used for X-ray diffraction studies. Metal and metal-oxide crystallite sizes were calculated from line-broadening data, as described elsewhere (*28*). The 400 diffraction line of η-Al_2O_3 was employed as an internal standard when relative metal sintering rates were calculated.

Transmission electron microscopy measurements. Electron microscopy studies were performed on a Philips EM300 transmission electron microscope, as described by Prestridge and Yates (*29*). Reduced Ir/Al_2O_3 model film catalysts were subjected to the following sequential calcination (20% O_2/He) treatments: (i) 500°C for 1 hr, (ii) 600°C for 30 min, and (iii) 700°C for 20 min. A number of samples were removed from the tube furnace after each treatment and examined. About half of the samples removed after (ii) were given an additional treatment. This consisted of spraying each with a fivefold excess of $Ba(NO_2)_2$ over Ir, calcining under 20% O_2/He (500 cc/min) at 550°C for 4 hr, and then reducing under 20% H_2/He (500 cc/min) at 500°C for 1 hr. Finally these samples were calcined under 20% O_2/He (500 cc/min) at 600°C for 30 min and then reexamined.

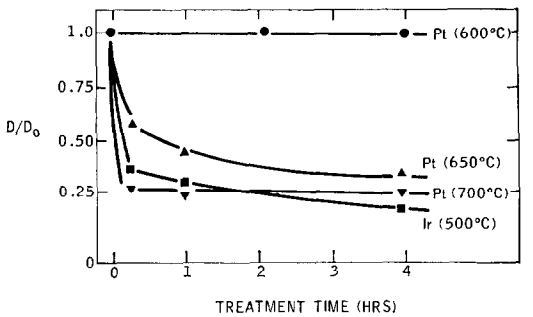

FIG. 2. Sintering behavior of 0.3% Pt and 0.3% Ir on Al_2O_3 catalysts under 20% O_2 at selected temperatures: H_2 chemisorption measurements.

Controlled atmosphere electron microscopy measurements. The technique of controlled atmosphere electron microscopy has been described elsewhere (*30*). CAEM enables one to follow continuously the behavior of a solid when it is heated in a gaseous environment. Model catalyst pretreatment was carried out as follows within the electron microscope gas cell: (i) calcining under 5 Torr oxygen at 250°C for 4 to 16 hr followed by (ii) reduction under 2 Torr hydrogen at 500°C for 1 hr. Such pretreated Ir/Al_2O_3 and $Ir/BaO–Al_2O_3$ model catalysts were examined under three different experimental conditions. These were (i) an experiment designed to measure the sintering rate of Ir on Al_2O_3 under 5 Torr oxygen over the temperature range of 400 to 750°C, (ii) an experiment designed to examine the effect of BaO on the oxidative sintering rate of Ir over the same temperature range, and (iii) an experiment designed to ascertain the effect of reduction–oxidation cycles on the redispersion rate of a presintered $Ir/BaO–Al_2O_3$ catalyst. Under the above conditions one is directly observing the growth (redispersion) of IrO_2 crystallites.

Quantitative measurements of the changes in IrO_2 crystallite dimensions under the various conditions were made from photographs taken off the televised image display and magnified 100-fold. The results presented are based on at least three reproducible experiments in each series. Low electron beam intensities were used to minimize heating effects.

Support acidity measurements. The acidities of η-Al_2O_3 and Group IIA-oxide doped η-Al_2O_3 supports were determined by titration of the solids with a standardized *n*-butylamine/benzene solution in the presence of a Hammett indicator (dicinnamalacetone) (*31–32*).

RESULTS AND DISCUSSIONS

Chemisorption and X-Ray Diffraction Studies

Sintering behavior of Ir/Al_2O_3 catalysts. The oxidative sintering characteristics of 0.3% Pt/Al_2O_3 and 0.3% Ir/Al_2O_3 catalysts are compared in Fig. 2. Dispersions have been normalized with respect to the dispersions of the fresh catalysts, i.e., D/D_0 is the ratio of H/M values of sintered and fresh catalysts. An identical set of curves would have resulted if CO/M values were used. The initial dispersion of the 0.3% Pt/Al_2O_3 (H/Pt = 1.26) catalyst is not decreased following a 4-hr oxygen calcination at 600°C (H/Pt = 1.24). Calcinations at 650 or 700°C, however, produce substantial decreases in dispersion. At these temperatures most of the sintering occurs during the first 15 min of treatment. At 700°C the lined-out dispersion (H/Pt = 0.31) corresponds to a Pt crystallite size of about 36 Å (*33*). X-Ray diffraction patterns of these same samples clearly indicate the presence of substantially larger crystallites (250–300 Å). These results suggest that sintered Pt catalysts contain a bimodal distribution of Pt crystallites. The fresh 0.3% Ir/Al_2O_3 catalyst demonstrated an H/Ir ratio of 2.56. In our laboratories we have consistently observed H/Ir and CO/Ir values in excess of unity for fresh Ir/Al_2O_3 and Ir/SiO_2 catalysts. H/Ir values in the range of 1.8 to 2.6 are typically obtained for 0.3 to 2% catalysts. Engels *et al.*, have recently reported H/M values of ~2 when iridium was added to a Pt/Al_2O_3 catalyst (*34*). Such

observations are usually attributed either to hydrogen-spillover (*35*) or to multiple bonding of the adsorbate on the corner and edge atoms of well-dispersed metal crystallites (*36–37*). CO/Ir values of fresh Ir/Al_2O_3 samples are generally found to be lower (~30–40%) than the corresponding H/Ir values. The 0.3% Ir/Al_2O_3 catalyst was found to sinter at a much lower temperature than required for Pt/Al_2O_3 catalysts. An H/Ir ratio of 0.48 was exhibited by the Ir/Al_2O_3 catalyst following a 4-hr oxygen calcination at 500°C. This value corresponds to an average iridium crystallite size of approximately 23 Å. X-Ray diffraction line-broadening measurements of calcined Ir catalysts suggest, however, the presence of substantially larger (170–250 Å) crystallites. In contrast to Pt, which grows as the metal, Ir oxidatively sinters into IrO_2 crystallites. These observations are in good agreement with the known chemistry of these metals in the presence of oxygen at elevated temperatures (*38–40*). As was observed for Pt/Al_2O_3 catalysts, sintered Ir/Al_2O_3 catalysts contain a wide distribution of crystallite sizes. A quantitative description of the bimodal distribution of sintered Ir/Al_2O_3 catalysts will be presented in a later section detailing the results of TEM studies.

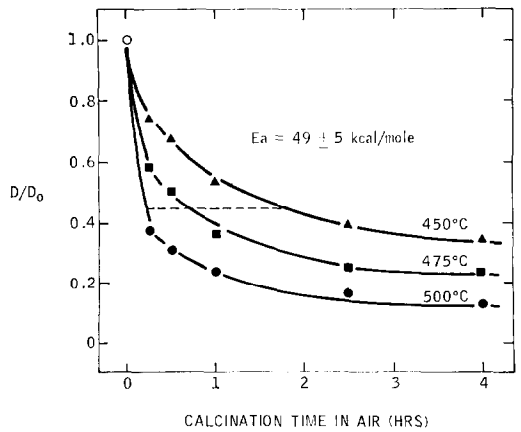

FIG. 3. Estimation of apparent activation energy for the oxidative sintering of a 1% Ir/Al_2O_3 catalyst: H_2 chemisorption measurements.

TABLE 1

Properties of Group IIA-Oxides/Al_2O_3 (520 μmole IIA Oxide/g Support)

Support	IIA Oxide (wt%)	BET (m^2/g)	Acidity (μmole/g)
η-Al_2O_3	—	217	325 ± 25
MgO/η-Al_2O_3	2.1	213	200 ± 25
CaO/η-Al_2O_3	2.9	218	0
SrO/η-Al_2O_3	5.4	224	0
BaO/η-Al_2O_3	7.9	209	0

If dispersion data at two or more temperatures as a function time are available and if the range of dispersions at the different temperatures overlap, it is possible to estimate an apparent activation energy for sintering (*41*). Such data obtained from hydrogen chemisorption studies are presented in Fig. 3. Taking values of Δt at the three temperatures at a constant D/D_0 of 0.45 and substituting into the following equation, one obtains a value for E_a of 49 ± 5 kcal/mole. Reference to this number will be made later.

$$E_a = R\left(\frac{T_1T_2}{T_2 - T_1}\right)\ln\frac{\Delta t_1}{\Delta t_2}$$

Sintering of Ir/Al_2O_3 catalysts in the presence of group IIA-oxides. Previously it was postulated that metal sintering under oxygen atmospheres might be suppressed or eliminated in the presence of an efficient chemical trap. Group IIA-oxides were suggested as potential trapping agents for Ir/Al_2O_3 catalysts. To test this theory, a series of Group IIA-oxide doped η-Al_2O_3 supports was prepared. Selected properties of these supports are summarized in Table 1. The mixed-oxide supports all exhibited BET surface areas comparable to those of the starting Al_2O_3. These supports showed no X-ray diffraction lines from either a Group IIA-oxide or an aluminate phase. The higher molecular weight Group

TABLE 2

Relative Agglomeration of 2% Ir Catalysts (From X-Ray Diffraction Measurements)[a]

IIA Oxide-Al_2O_3[b]	Relative agglomeration (%)	Known iridate
Al_2O_3	100	—
MgO/Al_2O_3	100	None
CaO/Al_2O_3	0	$CaIrO_3$
SrO/Al_2O_3	16	$SrIrO_3$
BaO/Al_2O_3	0	$BaIrO_3$

[a] Air treated for 4 hr at 500°C.
[b] IIA-Oxide/Ir = 5.

IIA-oxides were found to titrate completely the acid sites of the Al_2O_3 carrier. Since the acidic centers of Al_2O_3 are generally accepted to be well dispersed over the Al_2O_3 surface, the complete titration of these sites suggests that the basic oxides of Ca, Sr, and Ba are also well dispersed over the carrier surface. The MgO doped Al_2O_3 support was, however, found to retain considerable acidity, which suggests the preference of the smaller Mg cation to form a surface spinel.

To ascertain the ability of these mixed-oxide supports to stabilize the surface area of Ir, a series of 2% Ir catalysts was subjected to a 4-hr calcination at 500°C. The results of these tests are presented in Table 2. Under these conditions the oxides of Ca, Sr, and Ba were found to be very effective in suppressing the oxidative sintering of Ir. The MgO/Al_2O_3 support was not effective. Since Mg does not form an iridate, the inability of a MgO/Al_2O_3 support to suppress Ir sintering under oxygen lends credence to our iridate stabilization concept.

The suppression of sintering of Ir by Group IIA-oxide-Al_2O_3 supports indicated by X-ray diffraction measurements has been confirmed by H_2 and CO chemisorption. The results of a comparative CO chemisorption study are summarized in Fig. 4. The BaO doped catalyst exhibited an initial CO/Ir ratio of 1.14, which decreased only slightly to 1.03 following an 8-hr air calcination at 600°C. In the absence of BaO, the CO/Ir ratio dropped from an initial value of 1.32 to 0.15 after the same treatment. The remarkable stabilization of Ir surface area by the BaO/Al_2O_3 support was found to be maintained through six such oxidation–reduction cycles at 600°C.

The oxidative stabilization of Ir surface area was found to be critically dependent upon the Group IIA-oxide concentration. This dependence, shown in Fig. 5, suggests that stabilization of Ir is not achieved until the acidic sites of the Al_2O_3 support (325 μmole/g) are completely titrated with BaO. This behavior indicates that a strong acid–base interaction does not allow BaO to interact with Ir until the concentration of BaO is in excess of the Al_2O_3 acidity. This contention is supported in the case of a nonacidic SiO_2 support which requires a much lower BaO concentration to initiate Ir stabilization.

Redispersion of Ir/Al_2O_3 catalysts in the presence of group IIA-oxides. Under certain conditions the dispersion of $Ir/BaO–Al_2O_3$ catalysts was found to be increased by air calcination. Conditions under which redispersion can be achieved are outlined in Fig. 6. A partially sintered 1% Ir/Al_2O_3 catalyst was prepared by air calcining at 500°C for 2.5-hr. Upon reduction this catalyst was found to exhibit H/Ir and

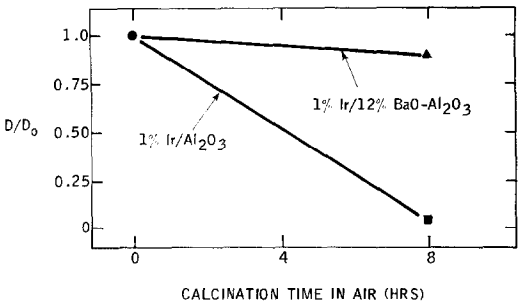

FIG. 4. Oxidative stabilization of Ir dispersion by a $BaO–Al_2O_3$ support (calcination at 600°C): CO chemisorption measurements.

CO/Ir values of 0.51 and 0.34, respectively. Sufficient aqueous $Ba(NO_2)_2$ was added at this point to produce a 12 wt% BaO phase. The $Ba(NO_2)_2$ doped catalyst was then air calcined at 550°C for 4 hr to ensure complete decomposition of the nitrite salt. After this treatment and a subsequent reduction step the catalyst demonstrated H/Ir and CO/Ir values of 0.32 and 0.23, respectively. Further air calcination at 600°C for 6 hr did not lower the Ir surface area. In the absence of BaO an Ir/Al_2O_3 catalyst treated as above would exhibit H/Ir and CO/Ir values of near 0.05. When the BaO-stabilized catalyst was reduced and then was air calcined again at 600°C for 6 hr, a marked increase in chemisorption was observed. When a reduction–calcination cycle was repeated three times while maintaining the total calcination time constant, an even larger increase in Ir surface area was obtained. Concomitant with the increased chemisorption of the latter sample was the complete loss of X-ray diffraction lines from a sintered Ir phase. Reduced Ir/Al_2O_3 catalysts were also found to sinter more extensively than samples not reduced prior to air calcination. An unreduced 1% Ir/Al_2O_3 catalyst which was air calcined at 500°C for 6 hr and then reduced exhibited an H/Ir ratio of 0.68. If the same starting catalyst is subjected to three reduction–calcination cycles with each cycle consisting

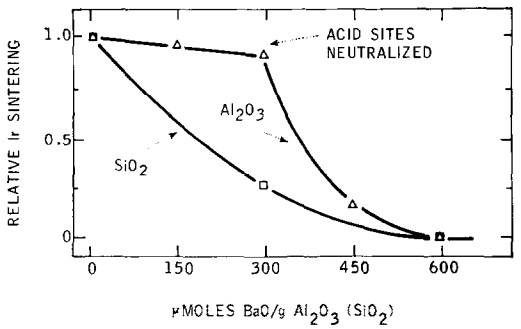

FIG. 5. Effect of BaO concentration on Ir surface area stabilization (air treated, 4 hr, 500°C, 150 μmole Ir/g): X-ray measurements.

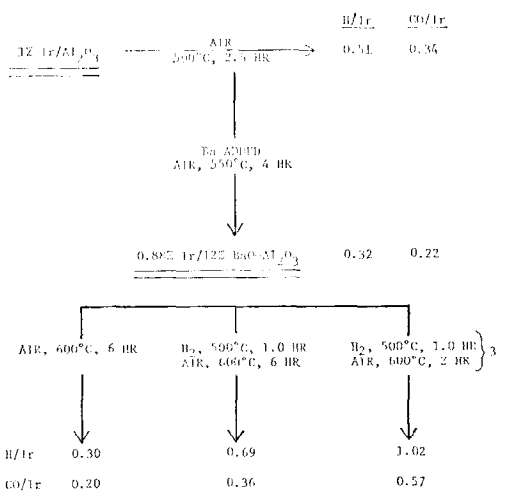

FIG. 6. Oxidative redispersion of supported iridium catalysts in the presence of BaO.

of a 0.5-hr hydrogen reduction at 500°C followed by a 2.0-hr air calcination at 500°C, the H/Ir ratio is lowered to 0.13. This corresponds to a fivefold increase in the extent of sintering over the catalyst not reduced prior to calcination. The increased rates of sintering and redispersion of Ir brought about by first reducing and then air calcining Ir/Al_2O_3 and $Ir/BaO–Al_2O_3$ catalysts suggest that mobile iridium oxide species are more readily generated from iridium metal crystallites than from IrO_2 crystallites. This suggestion is strengthened by considering the chemical transformations occurring during the chemical vapor transport of Ir under oxygen atmospheres (*38, 40*). The vapor transport of Ir is known to proceed by the generation of a gaseous IrO_3 intermediate. It has further been established that $IrO_{3\,(g)}$ is more readily generated from Ir metal than from IrO_2. The observed increase in dispersion in the above $Ir/BaO–Al_2O_3$ system is consistent then with the capture of molecular iridium oxide species (possibly IrO_3) by well-dispersed BaO traps, thereby producing immobile surface barium iridates. Subsequent reduction of the stable surface iridates thus yields a more highly dispersed Ir phase than present initially.

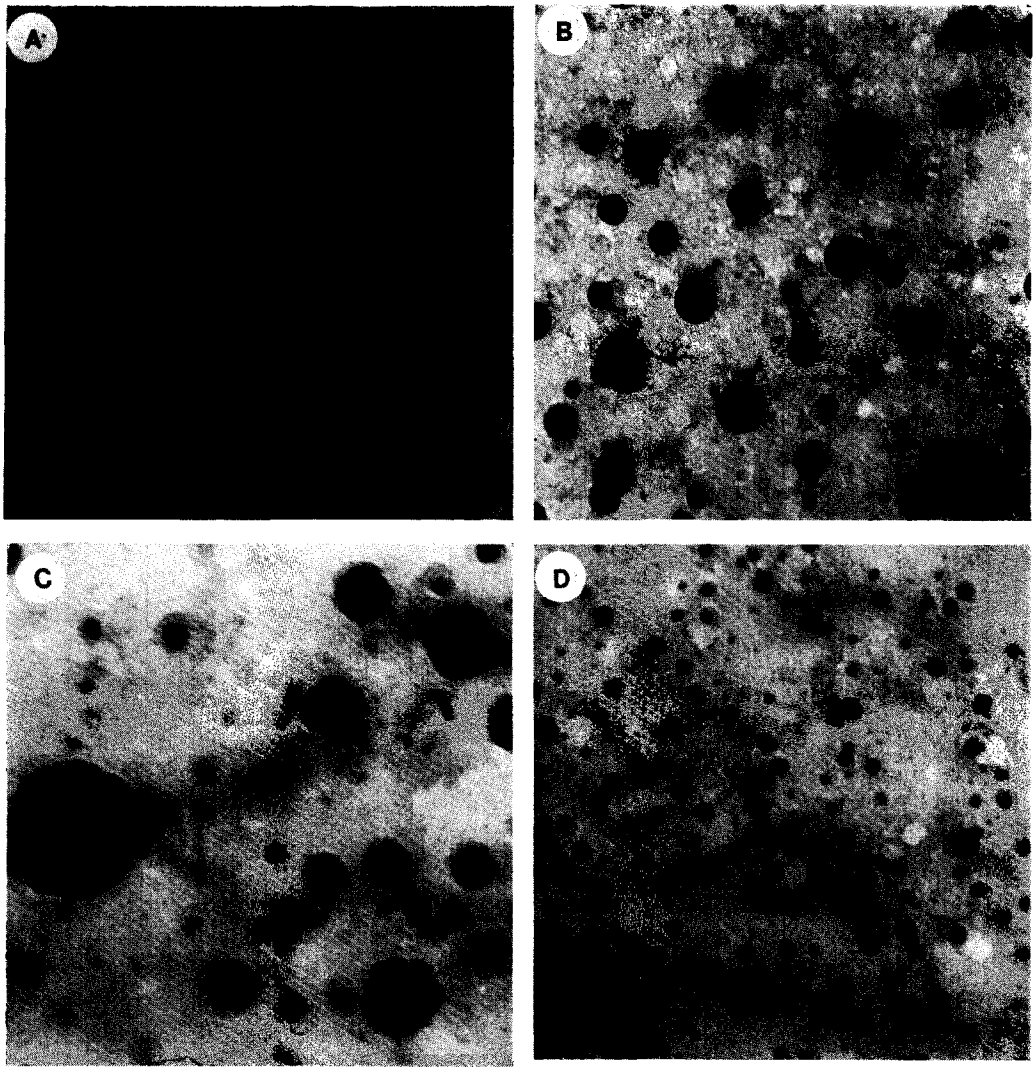

FIG. 7. Transmission electron micrographs of model Ir/Al_2O_3 and $Ir/BaO-Al_2O_3$ catalysts calcined under 20% oxygen. (A) Ir/Al_2O_3—500°C, 1.0 hr; (B) Ir/Al_2O_3—600°C, 0.5 hr; (C) Ir/Al_2O_3—700°C, 0.3 hr; and (D) prepared by doping (B) with BaO, reducing, and then recalcining at 600°C for 0.5 hr.

Transmission Electron Microscopy Studies of Model Ir/Al_2O_3 and $Ir/BaO-Al_2O_3$ Catalysts

Inspection of the electron micrographs of oxygen-calcined model Ir/Al_2O_3 catalysts, Figs. 7A to 7C, shows several interesting features. It is clear that the size of some of the IrO_2 particles increases appreciably over the range 500 to 700°C. A further feature is the presence of a large number of very small crystallites, <20 Å, in size. Finally, there is virtually no evidence in any of the micrographs of two particles interacting to give a "dumbbell" shape, which might be expected if particle growth occurred via a fusion of migrating crystallites.

Comparison of micrographs of specimens which were oxygen calcined at 600°C for 30 min (Fig. 7B) with those which were subsequently calcined for a further 30 min

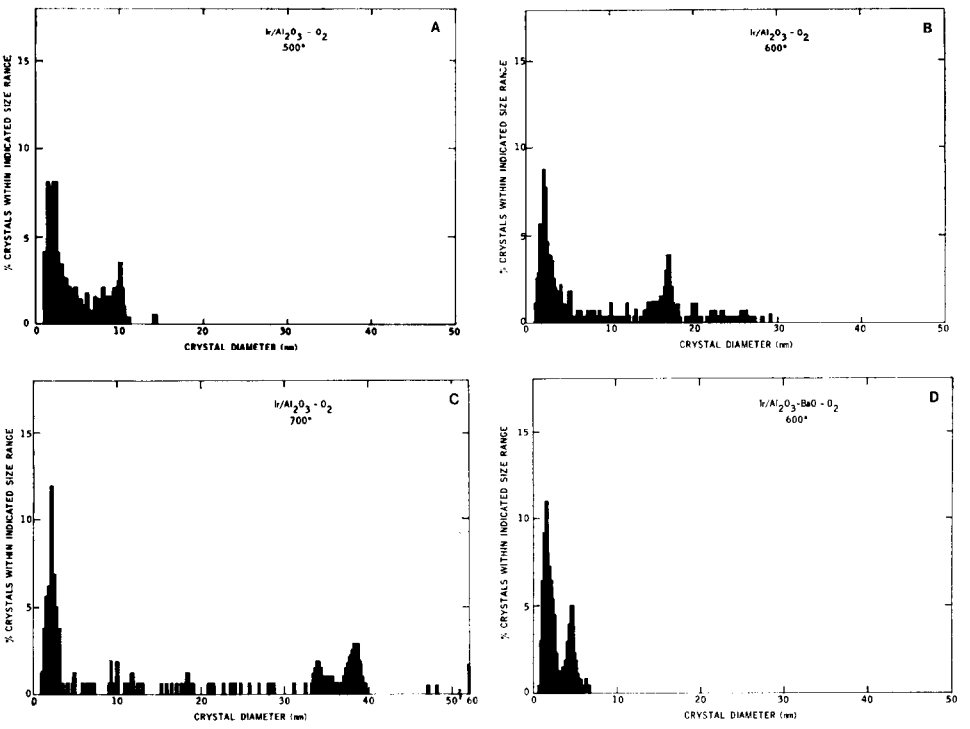

FIG. 8. (A–D) Particle size distribution curves obtained after the respective sample treatments outlined in Fig. 7.

at this temperature after first forming a BaO surface phase and then reducing (Fig. 7D) shows some profound differences in the sizes of the IrO_2 particles. We find that BaO not only has prevented further sintering, but also has induced considerable redispersion of the Ir component. In a separate experiment a sample of a BaO/Al_2O_3 support was calcined under oxygen at 700°C for 2.0-hr. Upon examination of this specimen no evidence of BaO particle formation was observed. We may therefore conclude that under the conditions used in these experiments one is only observing the growth of Ir in $Ir/BaO–Al_2O_3$ catalysts.

A more quantitative appreciation of the growth characteristics of Ir can be obtained from a detailed analysis of the crystallite size distribution after the various treatments, Figs. 8A to 8D. It is clear from these plots, which were obtained from measurement of over 500 particles after each treatment, that in calcined Ir/Al_2O_3 systems we are dealing with a bimodal distribution of IrO_2 crystallite sizes. The largest fraction of crystallites in all cases is between 10 and 30 Å. Comparison of Figs. 8A to 8C shows that as the temperature increases the separation between smallest and largest particles gets wider and the number of small crystallites formed increases. These findings are consistent with the notion that crystallite growth occurs by a molecular migration mechanism, which predicts that large crystallites increase in size at the expense of smaller crystallites.

The effect of added BaO on the growth of iridium crystallites can be seen from a comparison of Figs. 8B and 8D. Clearly BaO suppresses the growth process, probably by trapping migrating iridium oxide surface species. BaO, however, has little effect on the escape process of such species from the Ir crystallites so that the net effect is that

TABLE 3

Sintered Ir/Al_2O_3 Catalysts—A Comparison of X-Ray, H_2 Chemisorption, and TEM Measurements

T°C[b]	X-ray[c]	Crystallite size (Å)			H_2 chemisorption[c]
		TEM[a]			
		Min	Max	Av	
270	<50	<10	<10	<10	<10
500	173	<10	150	34	30
600	211	<10	280	68	62

[a] Model Ir/Al_2O_3 catalyst.
[b] Treatment time, 4 hr in air.
[c] 2% Ir/Al_2O_3 catalysts.

all crystallites decrease in size, i.e., redispersion occurs.

Average Ir crystallite sizes calculated from X-ray diffraction and H_2 chemisorption measurements on 2% Ir/Al_2O_3 catalysts and TEM measurements on a model Ir/Al_2O_3 catalyst system are compared in Table 3. The three methods all indicate that the fresh Ir/Al_2O_3 catalysts exhibit extremely well-dispersed iridium phases. After 500 and 600°C air calcinations, the average Ir crystallite sizes calculated from H_2 chemisorption data and observed in TEM measurements were found to be in very good agreement. The bimodal distribution of iridium crystallites causes X-ray line-broadening measurements to predict anomalously large average iridium crystallite sizes. Good agreement was observed between the largest IrO_2 crystallites seen in TEM micrographs and those calculated from X-ray line-broadening data. The generally good agreement in crystallite sizes determined by chemisorption measurements on conventional Ir/Al_2O_3 catalysts and TEM measurements on model Ir/Al_2O_3 catalysts strongly indicate the applicability of model systems in observing the sintering behavior of conventional catalysts.

Controlled Atmosphere Electron Microscopy Studies of Model Ir/Al_2O_3 and Ir/BaO–Al_2O_3 Catalysts

The use of CAEM enabled us to follow the growth of IrO_2 crystallites in real time. When reduced Ir/Al_2O_3 specimens were heated in 5 Torr O_2, the first signs of significant crystallite growth were observed at 440°C and appeared to slow down after about 2 hr. The largest IrO_2 crystallites present at this stage were about 100 Å in diameter. As the temperature was gradually raised to 750°C, several features of the crystallite growth process became apparent. The growth rate of IrO_2 crystallites increased and the time required to reach a limiting size decreased. The crystallites tended to be irregularly shaped and relatively dense. It was also noticeable that at any given temperature the crystallites were divided into two distinct size ranges, e.g., at 700°C about 5% of the particles were

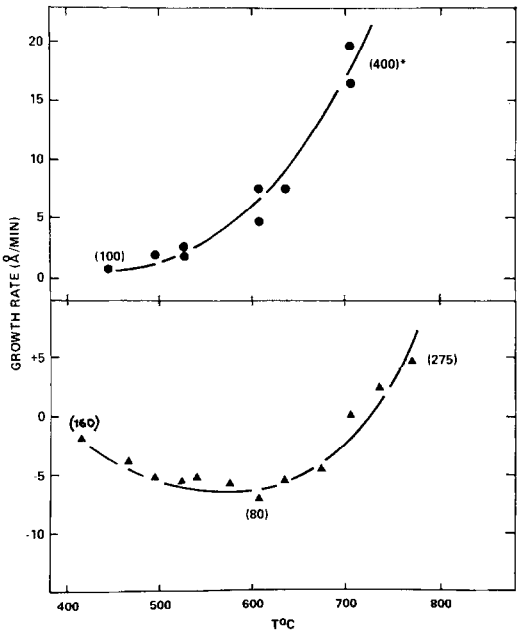

FIG. 9. Effect of oxidation (5 Torr O_2) on growth (redispersion) of Ir/Al_2O_3 (upper curve) and Ir/BaO–Al_2O_3 (lower curve) catalysts. The asterisk, * (numbers in brackets), indicates the largest particle size observed at a given temperature.

~400 Å in diameter, whereas the majority were <50 Å. Since the resolution of this technique is limited to 25 Å, precise quantitative estimates of IrO_2 crystallites below this size are not possible. During the growth sequences *no crystallite mobility was observed* and crystallites remained as discrete entities rather than tending to stick together in the form of dumbbells or chains.

Quantitative measurements were made from photographs taken during the periods where IrO_2 crystallites were growing at constant rates. These results are presented graphically in the upper half of Fig. 9. There is very good agreement between the sizes of the largest crystallite formed in these experiments with those found from X-ray and TEM investigations under similar calcination temperatures. This finding would appear to suggest that the partial pressure of oxygen does not have an appreciable effect on the extent of Ir sintering since there was a 30-fold difference in oxygen partial pressure between these investigations.

When similar experiments were performed on a presintered Ir/Al_2O_3 model catalyst in the presence of BaO, the behavior of the IrO_2 crystallites was quite different. Although the morphology of the particles was identical to that described above for the Ir/Al_2O_3 system, the growth

TABLE 4

Redispersion of Iridium Particles Supported on Alumina in the Presence of Barium Oxide After Reduction in Hydrogen At 500°C Followed by Oxidation in Oxygen At 600°C

Cycle No.	Redispersion rate (Å/Min)[a]	Largest particle size (Å)
0	—	250
1	−7.1	110
2	−4.15	25
3	−2.6	<25

[a] The redispersion rate (under 5 Torr O_2) was measured by CAEM.

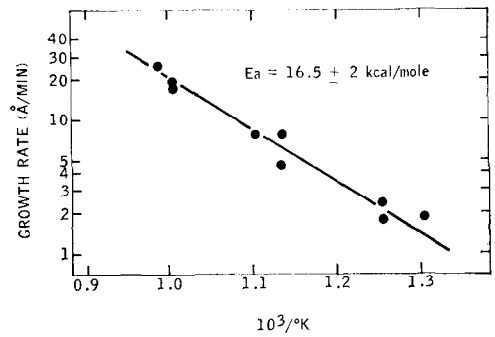

FIG. 10. Arrhenius plot for the oxidative (5 Torr O_2) growth of a Ir/Al_2O_3 catalyst.

characteristics of the crystallites changed dramatically. In this case the IrO_2 crystallites decreased in size when heated in oxygen over the range 417 to 672°C. At still higher temperatures some increase in size was observed, but the rate was drastically reduced compared to when BaO was absent. The effect of increasing temperature on this behavior appears to parallel that observed in the Ir/Al_2O_3 system, the time period over which crystallite shrinkage occurred becoming shorter as the temperature was raised. Quantitative measurements of this phenomenon are shown graphically in the lower half of Fig. 9, where it can be seen that the optimum conditions for redispersion are near 600°C.

The effect of treating $Ir/BaO–Al_2O_3$ specimens under three consecutive reduction–oxidation cycles where the oxidation step was maintained at 600°C is summarized in Table 4. It is apparent that consecutive treatments do bring about a reduction in crystallite size although the rate of redispersion decreases with each cycle. The size of crystallites listed is not the average size but rather those of the larger crystallites present, and after the third cycle these were below the resolution of the microscope (25 Å).

From the CAEM investigation several conclusions can be made, probably the most significant one being that in neither crystallite growth nor redispersion processes

were IrO_2 crystallites *observed to move on the Al_2O_3 surface,* which suggests that both these processes occur by a molecular migration mode. The introduction of BaO onto the Ir/Al_2O_3 system not only stabilizes the catalyst but also induces redispersion of large Ir crystallites, this process predominating at temperatures below 700°C and having the maximum effect at 600°C.

Recently Ruckenstein and Dadyburjor (*42*) have suggested that the failure to observe migration of crystallites in certain systems with CAEM (*43–44*) was due to a resolution limitation. Whereas this argument holds true for particles less than 25 Å in diameter, it has been demonstrated that in systems where crystallite migration occurs such motion is temperature dependent and as a consequence a temperature would be reached where IrO_2 particles larger than 25 Å would exhibit mobility (*45–46*). These conditions were never attained in the present investigation even though the sintering temperature was varied by 300°C. We must therefore conclude that crystallite migration does not play a role in the Ir/Al_2O_3–oxygen system at temperatures below 750°C.

The dependence of Ir sintering rate on temperature is presented in the form of an Arrhenius relationship in Fig. 10. From the slope of this line it has been possible to derive an apparent activation energy of 16.5 ± 2 kcal/mole for the growth of Ir on Al_2O_3 in the presence of oxygen. There is obviously a large difference between the activation energy obtained by this approach and that derived from chemisorption (49 ± 5 kcal/mole) measurements. The reason for this discrepancy becomes apparent when one considers the bimodal nature of the particle size distribution curves. It is clear that during sintering while some crystallites are growing a greater number are decreasing in size, and this effect leads to anomalous growth rates from a chemisorption approach. In CAEM studies one is actually measuring the growth of larger particles so this method removes any ambiguity and thus affords the true particle growth rate. It is interesting to compare the value of E_a of 16.5 kcal/mole obtained here with the value of 16 kcal/mole reported by Krier and Jaffee (*47*) for the evaporation of iridium forming $IrO_{3\ (g)}$ in fast flowing air. This agreement seems to imply that the sintering energetics of the Ir/Al_2O_3–oxygen system are governed by the generation of an iridium oxide species (possibly IrO_3) and not by the subsequent diffusion of such species over the support surface.

SUMMARY

Group IIA-oxides of Ca, Sr, and Ba have been found to stabilize the Ir surface area of Ir/Al_2O_3 catalysts under oxygen atmospheres at high temperatures. Oxidative stabilization is consistent with the formation of an immobile surface iridate via the reaction of a mobile, molecular iridium oxide species with a well-dispersed Group IIA-oxide. In support of this view, Mg, which does not form an iridate, was ineffective. The surface iridates are readily reduced to Ir metal and the corresponding Group IIA-oxide.

In the presence of a Group IIA-oxide, presintered Ir/Al_2O_3 catalysts can be redispersed under oxygen at relatively high temperatures. Redispersion most likely occurs by the formation of molecular iridium oxide species which migrate over the Al_2O_3 surface and ultimately become captured and immobilized by a well-dispersed Group IIA-oxide. Reduction of the stable surface iridate yields a more highly dispersed Ir phase than initially present.

Finally, CAEM measurements have clearly shown that Ir/Al_2O_3 catalysts sinter and $Ir/BaO–Al_2O_3$ catalysts redisperse under an oxygen atmosphere by a molecular migration mechanism. This finding is the first direct verification of the atomic

migration model outlined by Flynn and Wanke (*14*).

ACKNOWLEDGMENTS

The authors wish to thank Mr. N. C. Dispenziere, Mr. J. J. Eggert, Mr. R. D. Sherwood, and Mrs. L. W. Turaew for their valuable experimental assistance. A special thanks is extended to Dr. L. L. Murrell for measuring the acidity of the Group IIA–oxide–Al_2O_3 supports.

REFERENCES

1. Thomas, C. L., "Catalytic Processes and Proven Catalysts," Academic Press, New York, 1970.
2. Sinfelt, J. H., *Annu. Rev. Mat. Sci.* **2**, 641 (1972).
3. Mills, G. A., Weller, S., and Cornelius, E. B., "Proceedings of the Second International Congress on Catalysis," p. 2221. North-Holland, Amsterdam, 1961.
4. Boudart, M., Aldag, A. W., Ptak, L. D., and Benson, J. E., *J. Catal.* **11**, 35 (1968).
5. Dartiques, J., Chambellan, A., and Gault, F. G., *J. Amer. Chem. Soc.* **98**, 856 (1976).
6. Wanke, S. E., *J. Catal.* **46**, 234 (1977).
7. Granqvist, L. G., and Burhman, R. A., *J. Catal.* **46**, 238 (1977).
8. Wynblatt, P., *Acta Met.* **24**, 1175 (1976).
9. Bett, J. A., Kinoshita, K., and Stonehart, P., *J. Catal.* **35**, 307 (1974).
10. Ruckenstein, E., and Petty, C. A., *Chem. Eng. Sci.* **27**, 937 (1972).
11. Ruckenstein, E., and Pulvermacher, B., *Amer. Inst. Chem. Eng. J.* **19**, 356 (1973).
12. Wynblatt, P., and Gjostein, N. A., *Prog. Solid State Chem.* **9**, 21 (1975).
13. Flynn, P. C., and Wanke, S. E., *J. Catal.* **37**, 432 (1975); see also Jaworska-Galas, Z., and Wrzyszcs, J., *Int. Chem. Eng.* **6**, 604 (1966).
14. Flynn, P. C., and Wanke, S. E., *J. Catal.* **34**, 390 (1974).
15. Moore, W. J., "Physical Chemistry," p. 734. Prentice–Hall, Englewood Cliffs, N.J., 1965.
16. Geus, J. W., *in* "Chemisorption and Reactions on Metallic Films," (J. R. Anderson, Ed.), Chap. 3. Academic Press, London/New York, 1971.
17. Huang, F. H., and Li, C., *Scr. Metall.* **7**, 1239 (1973).
18. Wynblatt, P., and Gjostein, N. A., *Scr. Metall.* **7**, 969 (1973).
19. Newsome, J. W., Heiser, H. W., Russell, A. S., and Stumpf, H. S., "Alumina Properties," Aluminum Company of America, Pittsburgh, Pa., 1960.
20. Donohue, P. C., Katz, L., and Ward, R., *Inorg. Chem.* **4**, 306 (1975).
21. Rodi, F., "Untersuchungen an Erdalkalimolybdaten und-iridaten (IV)," Dissertation, Eberhard-Karl-Universität, Tübingen, Bundersrepublik, Deutschland, 1963.
22. Goodenough, J. B., and Longo, J. M., *in* "Landolt-Börnstein," New Series Group III (K. H. Hellwege and A. M. Hellwege, Eds.), Vol. 4, Part A, p. 132. Springer-Verlag, New York/Berlin, 1970.
23. Longo, J. M., private communication.
24. Analyses were performed by the Analytical and Information Division, Exxon Research and Engineering Company, Linden, New Jersey.
25. Benson, J. E., and Boudart, M., *J. Catal.* **4**, 704 (1965).
26. Wilson, G. R., and Hall, W. K., *J. Catal.* **17**, 190 (1970).
27. Yates, D. J. C., and Sinfelt, J. H., *J. Catal.* **8**, 348 (1967).
28. Klug, H. P., and Alexander, L. E., *in* "X-ray Diffraction Procedures for Polycrystalline and Amorphous Materials," 2nd ed., p. 687. Wiley, New York, 1974.
29. Prestridge, E. B., and Yates, D. J. C., *Nature (London)* **234**, 345 (1971).
30. Baker, R. T. K., and Harris, P. S., *J. Sci. Instrum.* **5**, 793 (1972).
31. Benesi, H. A., *J. Phys. Chem.* **61**, 970 (1957).
32. Bertolacini, R. J., *Anal. Chem.* **35**, 599 (1963).
33. Spenadel, L., and Boudart, M., *J. Chem. Phys.* **64**, 204 (1960).
34. Engels, S., Malsh, R., and Wilde, M., *Z. Chem.* **16**, 416 (1976).
35. Boudart, M., Vannice, M. A., and Benson, J. E., *Z. Phys. Chem. (N.F.)* **64**, 171 (1969).
36. Bobayashi, M., and Shirasaki, J., *J. Catal.* **28**, 289 (1973); **32**, 254 (1974).
37. Guerra, R. R., and Schulman, J. H., *Surface Sci.* **7**, 229 (1967).
38. Chaston, J. C., *Platinum Metals Rev.* **9**, 51 (1965).
39. Alcock, C. B., and Hooper, G. W., *Proc. Roy. Soc. Ser. A* **254**, 551 (1960).
40. Cordfunke, E. H. P., and Meyer, G., *Rec. Trav. Chim.* **81**, 670 (1962).
41. Wanke, S. E., *Catal. Rev. Sci. Eng.* **12**, 93 (1975).
42. Ruckenstein, E., and Dadyburjor, D. A., *J. Catal.* **48**, 73 (1977).
43. Baker, R. T. K., Thomas, C., and Thomas, R. B., *J. Catal.* **38**, 510 (1975).
44. Baker, R. T. K., and France, J. A., *J. Catal.* **39**, 481 (1975).
45. Baker, R. T. K., Harris, P. S., and Thomas, R. B., *Surface Sci.* **46**, 311 (1974).
46. Baker, R. T. K., and Skiba, Jr., P., *Carbon* **15**, 233 (1977).
47. Krier, C. A., and Jaffee, R. I., *J. Less Common Metals* **5**, 411 (1963).